



HAL
open science

Regression of primary hepatocarcinoma in cancer-prone transgenic mice by local interferon- γ delivery is associated with macrophages recruitment and nitric oxide production

Myriam Baratin, Marianne Ziol, Raphaëlle Romieu, Michèle Kayibanda, Fabrice Gouilleux, Pascale Briand, Pierre Leroy, Hedi Haddada, Laurent Renia, Mireille Viguier, et al.

► To cite this version:

Myriam Baratin, Marianne Ziol, Raphaëlle Romieu, Michèle Kayibanda, Fabrice Gouilleux, et al.. Regression of primary hepatocarcinoma in cancer-prone transgenic mice by local interferon- γ delivery is associated with macrophages recruitment and nitric oxide production. *Cancer Gene Therapy*, 2001, 8 (3), pp.193-202. 10.1038/sj.cgt.7700285 . hal-02427362

HAL Id: hal-02427362

<https://univ-tours.hal.science/hal-02427362>

Submitted on 4 Nov 2021

HAL is a multi-disciplinary open access archive for the deposit and dissemination of scientific research documents, whether they are published or not. The documents may come from teaching and research institutions in France or abroad, or from public or private research centers.

L'archive ouverte pluridisciplinaire **HAL**, est destinée au dépôt et à la diffusion de documents scientifiques de niveau recherche, publiés ou non, émanant des établissements d'enseignement et de recherche français ou étrangers, des laboratoires publics ou privés.

Regression of primary hepatocarcinoma in cancer-prone transgenic mice by local interferon- γ delivery is associated with macrophages recruitment and nitric oxide production

Myriam Baratin,¹ Marianne Ziol,² Raphaëlle Romieu,¹ Michèle Kayibanda,¹
Fabrice Gouilleux,³ Pascale Briand,⁴ Pierre Leroy,⁵ Hedi Haddada,⁶ Laurent Rénia,¹
Mireille Viguier,¹ and Jean-Gérard Guillet¹

¹Immunologie des Pathologies Infectieuses et Tumorales, INSERM U445, ICGM, Laboratoire associé n°9 du comité de Paris de la Ligue Nationale contre le Cancer, Paris, France; ²Service d'anatomie pathologie, hôpital Jean-Verdier and UPRES 1625, hôpital Avicennes, Bondy, France; ³Oncologie Cellulaire et Moléculaire, INSERM U363, ICGM, Paris, France; ⁴Génétique et Pathologie Expérimentales, INSERM U380, ICGM, Paris, France; ⁵Department of Immunobiology, TRANSGENE, SA, Strasbourg, France; and ⁶INSERM U362, IGR, Villejuif, France.

The clinical potential of tumor therapies must be evaluated using animal models closely resembling human cancers. We investigated the impact of locally delivered interferon- γ (IFN- γ) on primary hepatocarcinoma spontaneously developed by T-SV40 transgenic mice. A single intratumor injection of adenovirus IFN- γ was sufficient enough to induce *in vivo* production of biologically active IFN- γ , as assessed by STAT1 activation. IFN- γ secretion led to the regression of primary tumor, principally by apoptosis of tumor hepatocytes. The lack of T-cells infiltrates in the liver upon treatment excluded a role of a specific immune response. In contrast, indirect pathways may include tumoricidal function of macrophages. Indeed, they were massively recruited in the entire liver under IFN- γ treatment; transmigration through hepatic blood vessels could be observed and co-localization with damaged hepatocytes was obvious. This correlated with nonparenchymal liver cell iNOS expression and high level of NO in hepatic extracts. Moreover, *in vitro* experiments showed that NO releasing agents induced cell death of freshly isolated tumor hepatocytes, suggesting that NO could be one of the major effector molecules. Altogether, these observations defined an important role of IFN- γ in controlling tumor development in a model of primary hepatocarcinoma. **Cancer Gene Therapy (2001) 8, 193–202**

Key words: Hepatocarcinoma; gene therapy; interferon- γ ; apoptosis; macrophages; nitric oxide.

Since its discovery in the 1950s, numerous properties of Interferon- γ (IFN- γ) have indicated it to be a good candidate molecule for cancer therapy. IFN- γ is a pleiotropic cytokine essential for the generation of innate and cognate antitumor immune responses¹ by stimulation of tumor-specific CD8⁺ cytotoxic cells and direct activation of NK as well as macrophages tumoricidal properties. Moreover, IFN- γ is able to directly inhibit tumor cell growth, both *in vivo* and *in vitro*,^{2–4} as well as to down-regulate expression of angiogenic factors necessary for tumor growth and metastasis.^{4–7} Its role in tumor surveillance has been clearly demonstrated in mice that lack sensitivity to IFN- γ . Mice in which the expression of IFN- γ receptor or STAT1 have been inhibited are predisposed to enhanced tumor development induced by chemicals or when bred onto a p53^{-/-} background.⁸

These observations led us to investigate the role of IFN- γ in tumor development. To overcome deleterious side effects due to systemic administration of high doses of cytokines, we directly injected an IFN- γ recombinant adenovirus into the tumor site. As vectors, adenoviruses have several desirable properties including efficient transduction of a wide spectrum of proliferating or quiescent cells,⁹ and a major tropism for liver. Adenovirus IFN has been successfully used in several experimental tumor models.^{10–12} These models generally consist of tumor cell transplantation followed by adenovirus delivery or direct injection of recombinant adenovirus-transfected tumor cells. Nevertheless, as a rule, approaches successfully used with transplanted tumors may not be as efficient when applied to primary tumor models.¹³ We therefore chose to study a model of primary hepatocarcinoma that develops spontaneously. ASV-B mice are transgenic for the SV40 large T gene (T-SV40), which is under the control of the liver-specific antithrombin III promoter. Incidence of hepatocarcinoma occurs in 100% of the mice which die before 32 weeks of age.¹⁴ *In situ* delivery of adenovirus IFN- γ (Ad-IFN- γ) resulted in major destruc-

Received August 4 2000; Accepted December 22 2000.

Address correspondence and reprint requests to Dr. Myriam Baratin, INSERM U445, ICGM, Université René Descartes 27 rue du-faubourg-Saint-Jacques, Paris 75014, France. E-mail address: baratin@cochin.inserm.fr



tion of the primary hepatocarcinoma. Macrophages were massively recruited after treatment; transmigration through hepatic blood vessels as well as co-localization with damaged foci were observed. Further experiments suggested that nitric oxide (NO) may be the effector molecule responsible for tumor cells destruction. Indeed, iNOS production and NO increase were induced in IFN- γ -treated livers; moreover, freshly isolated tumor hepatocytes were very sensitive to this molecule.

MATERIALS AND METHODS

Mice

Production of transgenic ASV-B mice bearing SV40 early genes controlled by the antithrombin III liver-specific promoter on the Y chromosome has been previously described.^{14,15} These mice were extensively backcrossed with C57BL/6 J mice in the CNRS animal production facility (CDTA) at Orléans, France.

Recombinant adenovirus construction

Ad-IFN- γ is the AdTG6623 vector supplied by Transgène (Strasbourg, France) containing an intron between RSV promoter and IFN- γ cDNA. Mouse β -galactosidase cDNA was inserted into the padeno-RSV plasmid under transcriptional control of the RSV promoter. The construct contains flanking adenovirus sequences to promote homologous recombination. 293 cells were co-transfected with this plasmid along with dl324 *Clal*-digested DNA, which contains the E1-deleted adenovirus genome. Large-scale amplification of IFN- γ -positive clones was carried out by infecting 293 cells. Recombinant adenoviruses were harvested, purified by double cesium chloride gradient, dialyzed, and stored in 10% glycerol at -80°C . Viral stock titers were determined by plaque assay on 293 cells.

Infection of mice with recombinant adenoviruses

ASV-B mice were anesthetized and a small opening in the abdomen was made by cutting the skin just above the liver to visualize it through the peritoneum. In 100 μL of saline (or saline alone), 10^9 pfu of the adenovirus preparation was infused into the liver in a single injection. Finally, the skin was closed with a suture clip. Results reported herein integrate three independent experiments that have been grouped.

Liver protein extracts

Liver samples were harvested and maintained at $+4^{\circ}\text{C}$. For enzyme-linked immunoassay (ELISA), 400 μL of hypertonic buffer (HEPES pH 7.9 20 mM, NaCl 400 mM, EDTA 1 mM, DTT 1 mM, PMSF 1 mM, and the protease inhibitor cocktail) was used. Protein lysates were obtained by stirring the samples for 15 seconds at 10,000 rpm in a Polytron mixer. The homogenates were then centrifuged for 1 hour at $12,000\times g$ at $+4^{\circ}\text{C}$. Supernatants were harvested and protein concentrations evaluated using the Micro BCA Protein Assay Reagent Kit (Pierce, Rockford, IL).

Nonparenchymal liver cell protein extracts

Liver samples were harvested in phosphate-buffered saline (PBS) and rinsed several times to remove blood. Samples were minced with a razor blade and incubated at 37°C in collagenase containing buffer (NaCl 8 g/L, KCl 0.2 g/L, Na_2HPO_4 0.1 g/L, HEPES 2.38 g/L, CaCl_2 0.75 g/L, and collagenase H 0.5 g/L; Boehringer Mannheim, Mannheim, Germany) in a stirring bath for 30 minutes. Liver cells were separated by forcing pieces of liver through a 100- μm cell strainer (Falcon, Becton Dickinson, Franklin Lakes, NJ). Cell suspensions were centrifuged for 1 minute at $90\times g$ to eliminate cell debris. Pelleted cells were resuspended in PBS, layered onto 30% Percoll gradient, and centrifuged for 15 minutes at $600\times g$. Pellets containing nonparenchymal cells were resuspended and washed twice in cold PBS. Cells were then resuspended in a hypertonic buffer (HEPES pH 7.9 20 mM, glycerol 20%, NaCl 400 mM, EDTA 1 mM, DTT 1 mM, PMSF 1 mM, Leupeptin 5 $\mu\text{g}/\text{mL}$, and Aprotinin 5 $\mu\text{g}/\text{mL}$). The solution was immediately frozen in liquid nitrogen and thawed on ice. This step was repeated three times. Cell homogenates were then spun for 10 minutes at $12,000\times g$ and the supernatants harvested. Protein concentrations were evaluated with the Micro BCA Protein Assay Reagent Kit (Pierce).

Determination of IFN- γ level production

IFN- γ ELISA was carried out according to PharMingen (San Diego, CA) recommendations. The capture antibody (R46A2), detection antibody (biotinylated XMG1.2), and recombinant IFN- γ were purchased from PharMingen.

After boiling in loading buffer (Bio-Rad, Hercules, CA), each sample was loaded and separated on an 8% acrylamide gel. Proteins were electrophoretically transferred to a 0.45- μm pore size nitrocellulose membrane (Bio-Rad). Primary antibodies were incubated overnight at $+4^{\circ}\text{C}$ in PBS with 0.05% Tween 20 and 2.5% skim milk. Rabbit IgG anti-STAT1 antiserum (Upstate, Lake Placid, NY) was incubated at 1 $\mu\text{g}/\text{mL}$ and rabbit anti-iNOS antiserum (Alexis) at 1:2000. HRP-conjugated swine antirabbit IgG antiserum (Dako, Denmark) was added at a final concentration of 1:1000 for 1 hour. Probed proteins were detected with the Amersham (Buckinghamshire, England) Enhanced Chemiluminescence (ECL) system according to manufacturer's instructions.

Histology and immunohistochemistry

IFN- γ , CD4, and CD8 staining. Liver slides were snap-frozen in cold isopentane. Five-micrometer cryosections were cut and fixed in cold acetone. Endogenous biotin activity was blocked according to the Dako biotin-blocking system procedure. Biotinylated antibodies were incubated overnight at room temperature. Anti-IFN- γ (XMG1.2) was used at 2 $\mu\text{g}/\text{mL}$, anti-CD4 (GK1.5), and anti-CD8 (53-6.7) at 5 $\mu\text{g}/\text{mL}$. Reactions were developed with Streptavidin-PAL and with Fuchsin, as substrate, according to manufacturer's specifications (Dako). Finally, sections were counterstained with haematoxylin.

HES staining. Livers were harvested, fixed in AFA solution (ethyl alcohol 85%, formalin 10%, acetic acid 5%), and embedded in paraffin. Five-micrometer sections were cut, deparaffinized, rehydrated, and stained with haematoxylin, eosin, and saffron.

TUNEL staining. For apoptosis analysis, sections were prepared as described above and stained by the TUNEL method, according to the Apoptog *in situ* Apoptosis Detection Protocol (Oncor, Purchase, NY). Pretreatment consisted of microwaving the slides for 5 minutes in citrate buffer. Negative control sections were stained without the TDT enzyme. DAB (Sigma, St. Louis, MO) was used as the developing substrate and sections were counterstained with periodic acid, Shiff reactive, and Mayer's haematoxylin.

Macrophages staining. Five-micrometer paraffin sections were dewaxed in xylene and rehydrated. Slides were placed in a citrate buffer (10 mM, pH 6) and microwave-heated for 20 minutes at 650 W. Endogenous peroxidases were inhibited in methanol 3% H_2O_2 . Then sections were incubated with anti-Mac 2 (TIB 166, ATCC, Bethesda, MD) antibody (supernatant of the hybridoma diluted at 1:4) and subsequently with peroxidase conjugate rabbit antirat (Dako) at a final dilution of 1:2000. Staining was amplified using StreptABComplex/HRP Duet, Mouse/Rabbit (Dako) according to manufacturer's instructions. Finally, slides were counterstained with Mayer's haematoxylin before mounting.

Quantification of macrophages infiltration and area of cell destruction by image analysis

Analysis of each slides was performed using a mono CCD color video camera (SONY Exwave HAD) mounted on top of a light microscope (Olympus BX40) attached to a soft imaging system, ANALYSIS (Münster, Germany).

A $\times 200$ magnification was used for quantification of the total surface occupied by $\text{Mac}2^+$ cells. In each tissue specimen labeled with anti-Mac2, 10 fields outside destroyed areas were selected and digitized for analysis. The computer segmentation of the positively stained areas was based on the range threshold of the green component of the RGB image. The reproducibility of the analysis was controlled by comparison of analysis of elementary fields measured through various lenses and by iterative measurements. Results were expressed as mean immunostained fractional areas.

A $\times 20$ magnification was used for tissue destruction assessment. Tissue sections were entirely digitized and boundaries of destruction areas were manually traced using the image analysis software. Results are expressed as mean fractioned area for each animal.

Evaluation of NO_2^- concentration

The nitrate in samples was converted to nitrite with *Aspergillus niger* nitrate reductase (Boehringer Mannheim). Briefly, an aliquot (50 μL) of hepatic homogenate was incubated for 20 minutes at room temperature with 5 μL of nitrate reductase, 15 μL of β -nicotinamide dinucleotide phosphate (Sigma), and 10 μL of flavin adenine dinucleotide (Sigma). Reduced samples were incubated with 10 μL

of Griess reagent [1% sulfanilamide (Sigma), 0.1% naphthylenediamine chloride (Sigma) in 2.5% H_3PO_4] and 100 μL of trichloroacetic acid (10% aqueous solution). Samples were centrifuged at 15,000 rpm for 15 minutes and each supernatant was placed in the wells of a 96-well (flat bottom) plate (Costar, Cambridge, MA). The absorbance at 540 nm was measured. Nitrate concentrations were determined using NaNO_3 as standard.

In vitro assay hepatocytes sensitivity to NO

Mouse hepatocytes were isolated by a two-step collagenase perfusion of liver fragments and were further purified over a 30%, rather than the usual 60%, Percoll gradient. Indeed, size of tumor hepatocytes is heterogenous and rather small so that a 60% Percoll gradient resulted in cell loss. Twenty thousand cells were seeded into 96-well flat bottom microplates in William's medium (Gibco, Edinburgh, Scotland) supplemented with 10% fetal calf serum, 2 mM glutamine, and antibiotics. They were then allowed to adhere for 24 hours in 3.5% CO_2 at 37°C and rinsed with new culture medium before treatment. NO releasing agents, SNP (sodium nitroprusside) and DEA/NO ($(\text{C}_2\text{H}_5)_2\text{N}[\text{N}(\text{O})\text{NO}]^-\text{Na}^+$), were added for 24 hours in 100 μL medium to give a final concentration of 313–5000 μM . Hepatocytes were also incubated in medium alone as a control. Cell viability was evaluated by a MTT assay: MTT at 0.5 mg/mL (Sigma) was added to each well and the plates were incubated for another 4 hours at 37°C . MMT is a pale yellow substrate that becomes a dark blue formazan product when incubated with live cells. The blue crystals of formazan were dissolved in 100 μL of a 50/50 ethanol/DMSO mixture. Absorbance (A_x) was then read at 560 nm. Results are expressed as percentage of viability, V_x , $V_x = 100[(A_x - A_0)/(A_{\text{max}} - A_0)]$, with A_0 being the absorbance obtained in absence of hepatocytes and A_{max} the absorbance obtained in the absence of NO releasing agents.

RESULTS

A single intratumor injection of Ad- $\text{INF-}\gamma$ resulted in vivo production of biologically active $\text{INF-}\gamma$

To evaluate the impact of $\text{INF-}\gamma$ expression on hepatocarcinoma progression, we injected 10^9 pfu of recombinant adenovirus directly into the livers of ASV-B transgenic mice. Mice were treated with a single injection at 4 months of age, at a time point when tumor growth was maximal and the liver presented a well-differentiated hepatocarcinoma.¹⁵ Control mice were injected either with adenovirus- β -galactosidase (Ad- β -gal) or saline. Mice were sacrificed 7 days later. Indeed, data from pilot experiments designed to study pharmacokinetics of $\text{INF-}\gamma$ production showed that $\text{INF-}\gamma$ was rapidly expressed and already detected at an important level from day 3. The maximum was reached at day 7; from then on, the level tapered very quickly and returned to baseline at day 15.

Blood samples were drawn before injection, 4 days after, and at the day of sacrifice. ELISA analysis of serum and liver homogenates revealed massive $\text{INF-}\gamma$ produc-

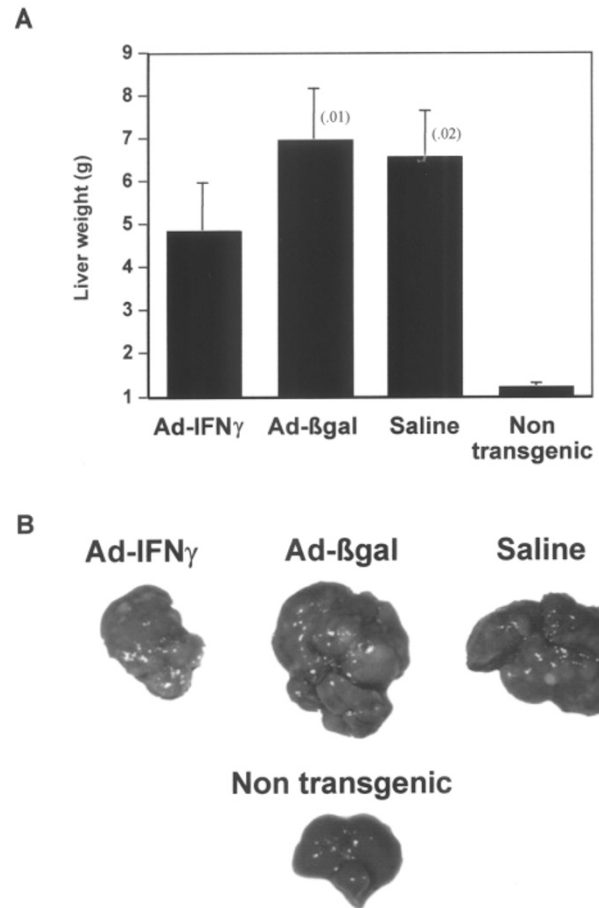
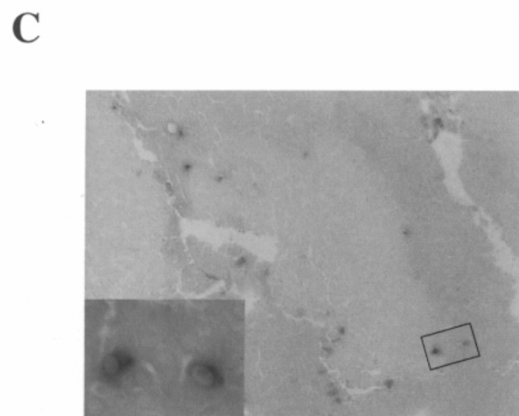
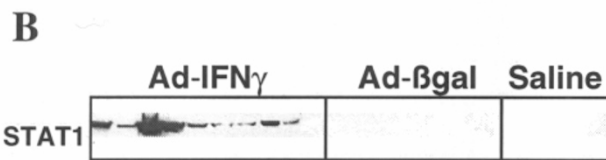
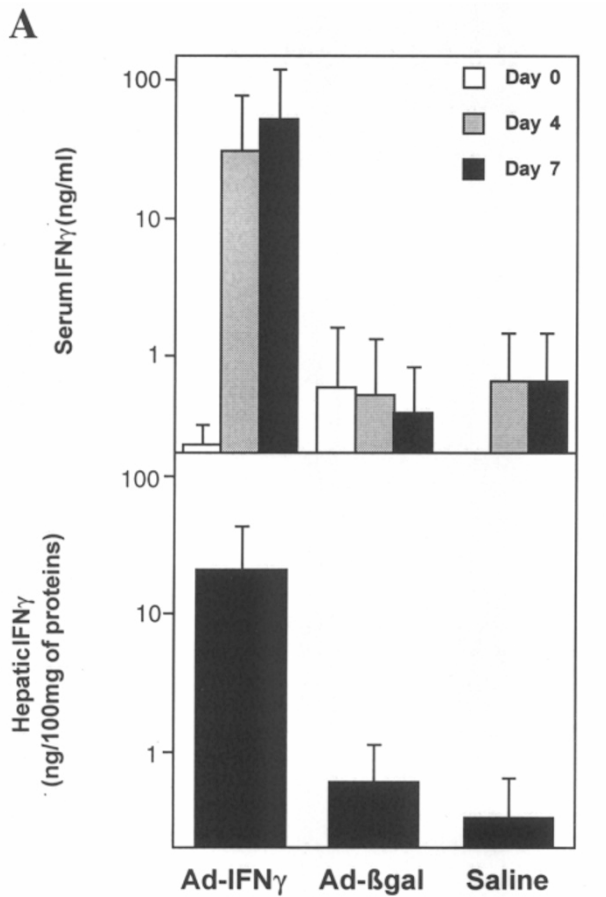


Figure 2. Evaluation of tumor regression. Livers of treated mice were harvested and weighted (A). Means of each group are represented on the graph. Ad-IFN- γ -treated mice were individually compared with the saline and Ad- β -gal groups using the Mann-Whitney *U* test. Statistical significance is indicated on the graph. Nontransgenic liver weights are also presented as healthy control. Livers were photographed in order to visualize macroscopic appearance of hepatocarcinomas. One representative liver of each group is presented (B).

tion only in Ad-IFN- γ -treated mice (Fig 1A). At day 4, seric IFN- γ level was already 30 times higher in those

Figure 1. Production of biologically active IFN- γ . Serum and hepatic IFN- γ productions were determined (A). Animals received a single intratumoral injection of either 10^9 pfu Ad-IFN- γ ($n=10$), 10^9 pfu Ad- β -gal ($n=7$), or saline ($n=4$). Postinjection, sera were collected on days 0, 4, and 7 (day of sacrifice) and IFN- γ concentrations determined by ELISA. On day 7, hepatic homogenates were prepared as described in the experimental procedures. Hepatic expressions of IFN- γ were assessed by ELISA. Results are expressed as nanograms of IFN- γ per 100 mg of total proteins. STAT1 expression in liver was evaluated (B). Liver homogenates were prepared and STAT1 expression determined by Western blot. One hundred fifty micrograms of each sample was loaded onto an 8% acrylamide gel. Liver tissue section of Ad-IFN- γ -treated mouse was stained with anti-IFN- γ (C). Pictures showed that only a few hepatocytes were positively stained and that they were mainly distributed around damaged areas (original magnifications: $\times 100$ and $\times 1000$).

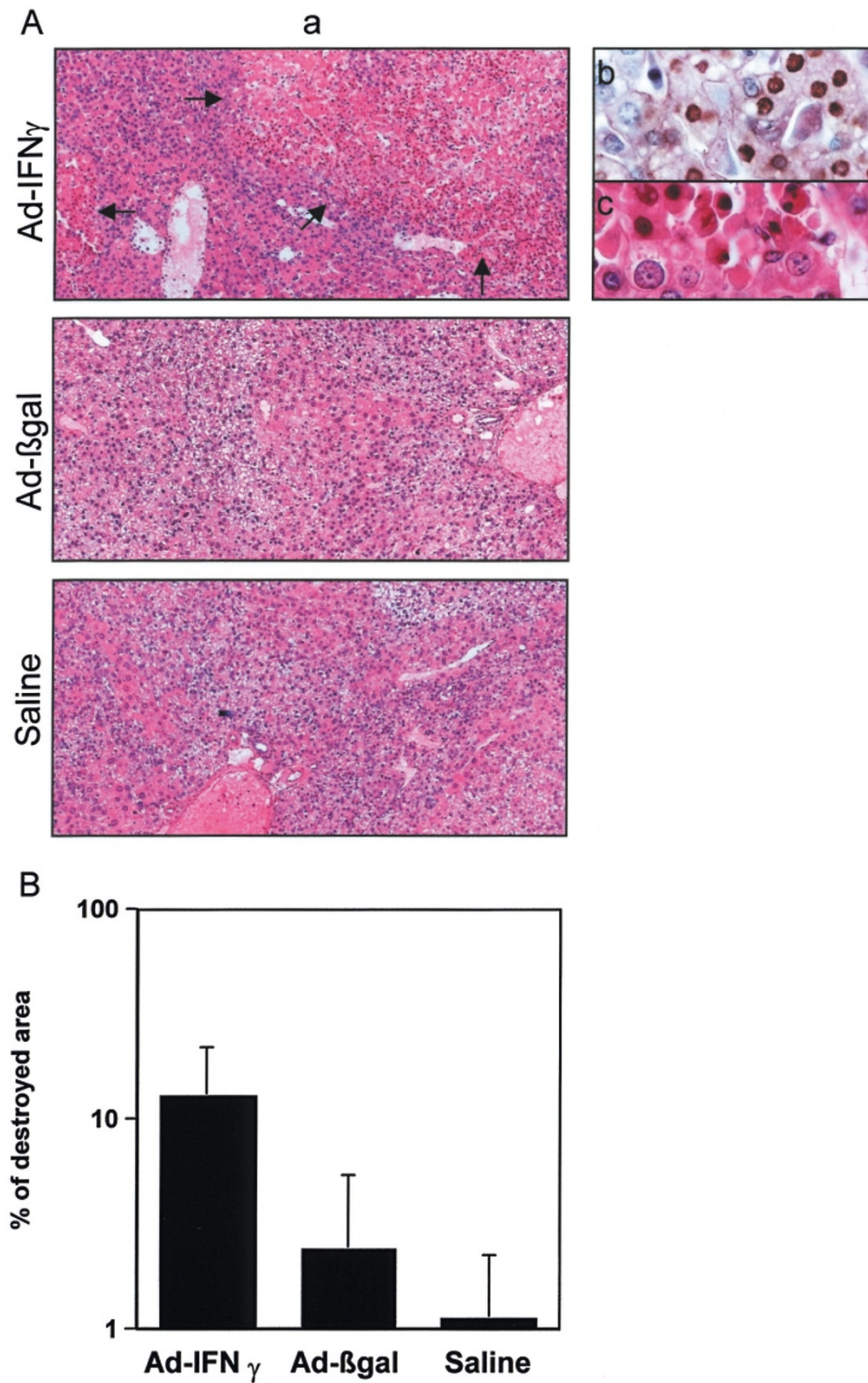


Figure 3. Large areas of tumor destruction in Ad- $\text{INF-}\gamma$ -treated animals. HES-stained liver sections of a representative animal in each group is shown at $\times 100$ original magnification (**A, a**). Arrows indicate areas of tumor cell death. Higher magnification ($\times 1000$) of destroyed areas shows cytoplasmic condensation and nuclear fragmentation characteristic of apoptotic cell death (**A, c**). Apoptosis was further confirmed by TUNEL staining (**A, b**). The extent of tumor destruction was quantitatively assessed by image analysis and expressed as percentage of destroyed area on the total surface (**B**).

mice than those in the control; this ratio reached 50 on day 7. In hepatic extracts, this increase was also obvious

with a ratio closed to 20. No significant difference could have been established in saline- and Ad- β -gal-treated

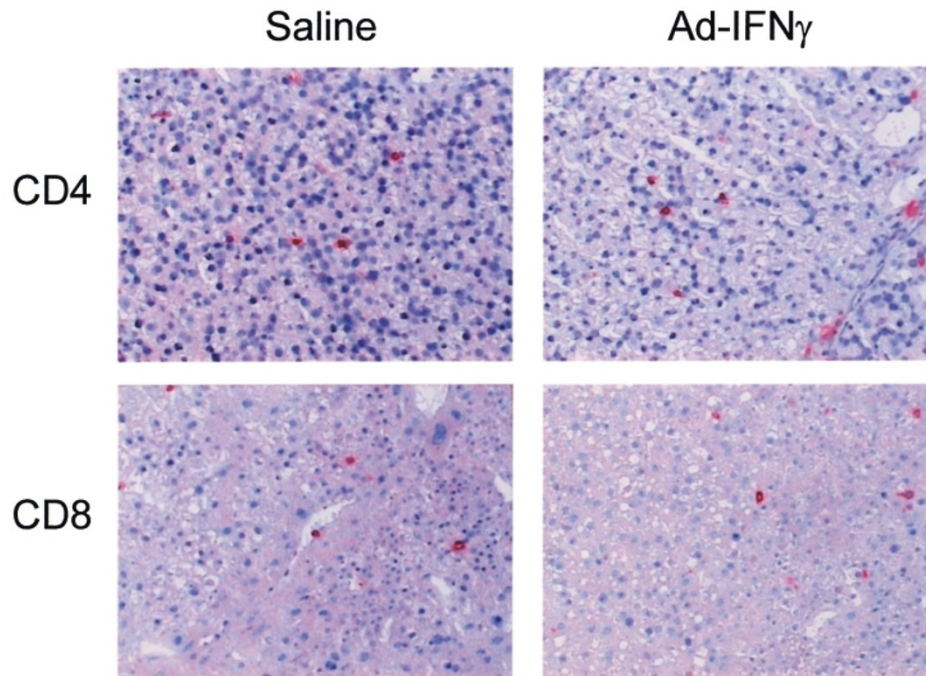


Figure 4. No T-cell infiltrates were detected on liver section at time of sacrifice. Tissue sections were stained with anti-CD4 and anti-CD8. A $\times 100$ magnification of Ad-IFN- γ - and saline-treated mice sections showed the absence of infiltrates at time of sacrifice; numbers of positive cells were very similar in each case.

mice; thus, IFN- γ expression was mostly due to the transgene and not from the adenovirus particle by itself.

Immunostained frozen liver sections revealed that IFN- γ was mainly produced by hepatocytes (Fig 1C). Interestingly, this staining showed that although only a few hepatocytes secreted the transgene protein, it was sufficient to produce a high cytokine level (Fig 1A and B). This observation is consistent with the reported results of Qin et al¹⁶ reporting that as few as 1% adenovirus IFN- β -transfected cells could block tumor growth after implantation.

To investigate the biological activity of IFN- γ , we evaluated the production of STAT1, a specific IFN- γ signaling factor in liver homogenates by Western blot. Figure 1B shows that IFN- γ production in serum and liver was accompanied by the appearance of STAT1 protein (9 of 10 Ad-IFN- γ -treated animals). Any of the control animals did not produce detectable levels of this protein. Moreover, STAT1 phosphorylation was assessed in four IFN- γ -treated liver homogenates and established by Western Blot (data not shown), meaning that the protein was activated.

IFN- γ production resulted in the regression of the hepatocarcinoma

To evaluate the impact of IFN- γ production on mouse liver tumor, we weighed the livers of animals after sacrifice (Fig 2A). The tumor weight is virtually the liver weight of ASV-B transgenic mice because transformed hepatocytes completely invade this organ. Mean liver weight of IFN- γ -

treated animals was statistically reduced, compared to control mice (P was equal to .01 and .02 when compared, respectively, with Ad- β -gal- and saline-treated mice; Figure 2A). However, the macroscopic appearance of IFN- γ -treated livers did not return to normal. The only clear differences at the sacrifice were the reduction of tumor volume (Fig 2B) and the macroscopic emergence of destroyed areas.

Destruction of hepatocarcinoma was principally due to tumor cell apoptosis

To analyze tumor regression, HES-stained liver sections were examined, revealing large areas of tumor cell destruction in the majority of Ad-IFN- γ -treated livers (Fig 3A, a). These regions were randomly distributed throughout tumor nodules and no vascular systematization was found. Examination of these destroyed areas revealed damaged tumor cells exhibiting cytoplasm and chromatin condensation as well as nuclear fragmentation characteristic of apoptosis (Fig 3A, c). These cells also demonstrated intense nuclear staining with the TUNEL method (Fig 3A, b). In contrast, control livers did not show such a destruction (Fig 3A,a). Examination of TUNEL-stained section also showed that positive cells were mainly hepatocytes and that no endothelial cells were labeled (data not shown).

Percentage of destroyed areas was evaluated by image analysis (Fig 3B). A clear correlation was observed between serum IFN- γ production and tumor destruction ($r^2=0.8$,

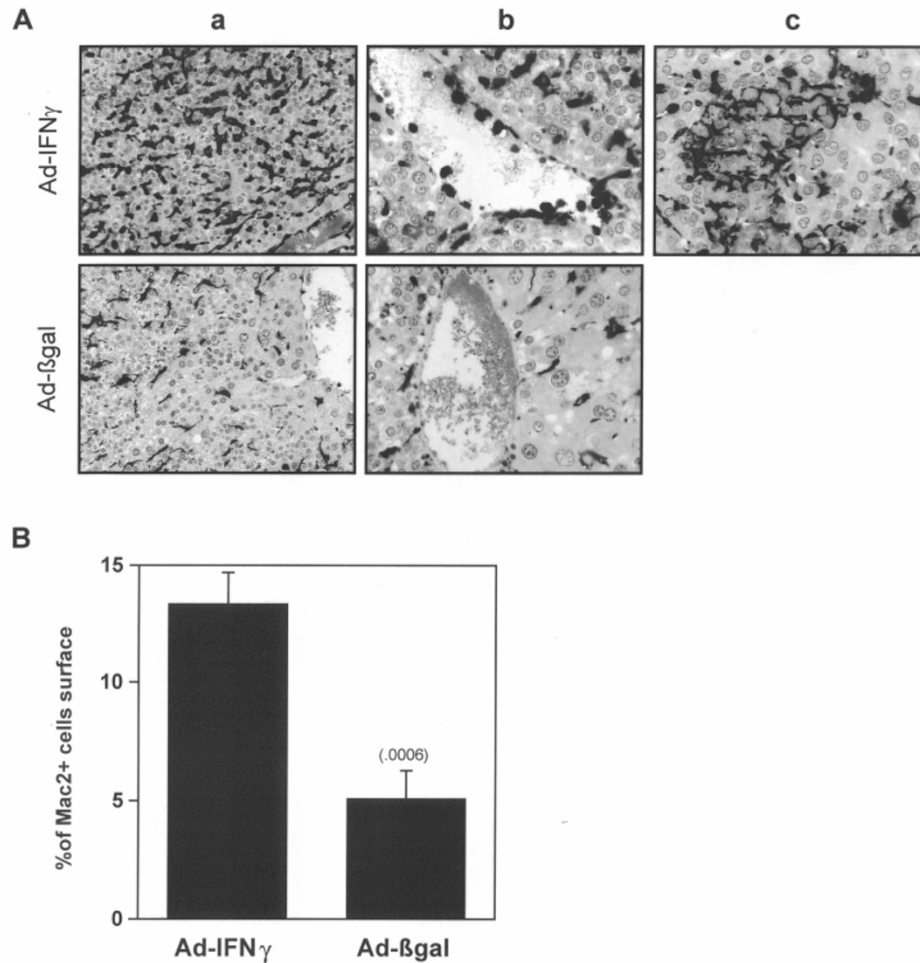


Figure 5. Macrophages recruitment following intrahepatic Ad-IFN- γ injection. Tissue sections were labeled with anti-Mac2. A $\times 200$ magnification of nondestroyed liver parenchyma showed the presence of macrophages regularly distributed throughout hepatic tissue of Ad-IFN- γ - and Ad- β -gal-treated mice (**A, panel a**). Upon Ad-IFN- γ treatment, an increase of these cells was clearly observed and established by image analysis (**B**). Ad-IFN- γ -treated group was compared with Ad- β -gal group using the Mann-Whitney U test. Statistical significance is indicated on the graph. A $\times 400$ magnification of intratumor blood vessels is also presented and showed obvious transmigration of Mac2 $^{+}$ cell in a Ad-IFN- γ -treated mice (**A, panel b**). Finally, Mac2 $^{+}$ cells were observed in areas where damaged tissues were in a Ad-IFN- γ -treated liver (**A, panel c**, $\times 400$ magnification).

$P=.0001$). Mean of destruction was 5-fold higher in Ad-IFN- γ -treated animals than in control ones, in which destruction was basal.

In additional experiments with nontransgenic littermates that received Ad-IFN- γ and consequently expressed STAT1 in the liver, we were unable to detect massive liver destruction. Few apoptotic cells were found in the liver of such animals, but they were isolated and distributed uniformly throughout the liver sections (data not shown). This suggested that only tumor liver was destroyed by IFN- γ .

Modulation of macrophage tumoricidal activity

To study whether Ad-IFN- γ generates tumor destruction directly or through the recruitment of effector cells, different stainings were performed on liver tissue sections. No CD4 or CD8 T-cells infiltrates were detected at the time of sacrifice; number of T cells in Ad-IFN- γ -treated mice was low and

similar to control animals (Fig 4). Examination of anti-Mac2 stainings revealed positive cells regularly distributed throughout hepatic sinusoids in all animals. However, the proportion of these cells was greatly enhanced and invaded the liver tissues in Ad-IFN- γ -treated mice (Fig 5A, a). Quantitative assessment by image analysis outside destroyed areas showed a 2- to 3-fold increase (Fig 5B). Moreover, transmigration of macrophages seemed to occur. Indeed, as shown in Figure 5A, b great amounts of Mac2 $^{+}$ were observed in and around hepatic blood vessels as well as inside the vessel wall. Finally, destroyed foci were often massively infiltrated and bordered by these cells (Fig 5A, c). In contrast, control animals did not present any of these particularities.

To evaluate the tumoricidal potential of these recruited macrophages, iNOS was assessed in total liver homogenates, but remained undetectable by Western blot. However, in nonparenchymal cells preparation free of



hepatocytes, significant production of iNOS was observed in Ad- $\text{INF-}\gamma$ -treated livers (Fig 6A). This expression was associated with increased seric (data not shown) and hepatic NO concentrations as evaluated at the time of sacrifice (Fig 6B).

Tumor hepatocytes showed a marked NO sensitivity in vitro

To assess the hypothesis that NO is one of the effector molecules responsible for tumor cell destruction, we isolated and purified hepatocytes from 3-month-old ASV-B mice as well as from control littermate and tested their sensitivity to SNP and DEA/NO, NO releasing agents. These compounds release NO as soon as they are in solution. In the absence of NO donors, no cell death was induced in normal or in tumor hepatocytes. This result proved the absence of endogenous toxic agents, which could have contaminated hepatocytes cultures. In that context, nature of hepatocytes was the only variable and NO the only reactive agent. Viability of tumor hepatocytes was greatly reduced upon NO donors treatment (Fig 7). Moreover, a differential sensitivity was observed between

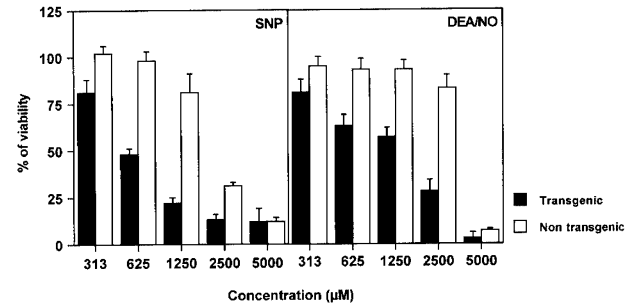


Figure 7. Marked sensitivity of tumor hepatocytes to NO. Hepatocytes were isolated by collagenase perfusion of liver biopsy from transgenic and nontransgenic mice. They were seeded in 96-well flat bottom microplates at 20,000 and then allowed to adhere for 24 hours in 3.5% CO_2 at 37°C. After this time, various concentrations of SNP and DEA/NO were added. After another 24 hours, cell viability was assessed by the MTT test. Results are expressed as percentage of maximal viability obtained in the absence of NO donors (see *Materials and Methods*).

tumor and normal hepatocytes for which viability was two to three times higher.

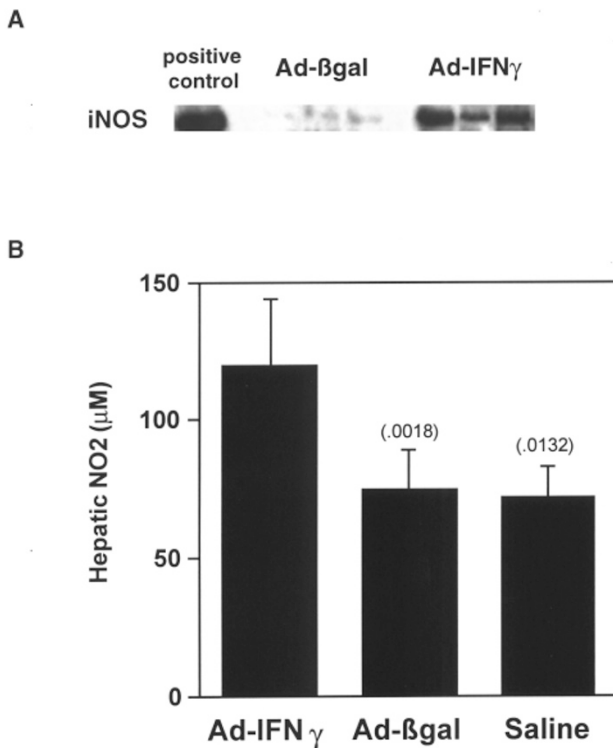


Figure 6. Detection of iNOS and NO_2^- in the liver. iNOS expression was evaluated by Western blot in protein extracts (40 μg) from nonparenchymal liver cells of 3 Ad- $\text{INF-}\gamma$ - and 3 Ad- β -gal-treated mice (A). The positive control is a protein extract of adherent cell-enriched splenocytes stimulated for 24 hours with LPS (30 μg/mL) and $\text{INF-}\gamma$ (40 U/mL). Hepatic NO in all animals was evaluated by measurement of NO_2^- concentration (B). Ad- $\text{INF-}\gamma$ -treated group was compared individually with saline and Ad- β -gal groups using the Mann-Whitney U test. Statistical significance is indicated on the graph.

DISCUSSION

A critical function of animal tumor models is to evaluate the safety and therapeutic efficacy of anticancer strategies. Most animal tumor models use grafted syngeneic tumor cells. Whereas they may be informative and lead to an understanding of specific immune responses, they can be misleading in predicting outcomes of clinical trials. In contrast, the primary tumor model of ASV-B mice used in this study is probably more representative of spontaneous cancers arising in human. Indeed, the oncogenic transgene T-SV40 could be assimilated to a self-antigen. Furthermore, because it is placed under the control of antithrombin III liver-specific promoter, it could be considered as a differentiation tumor antigen such as tyrosinase, Melan/MART-1, or gp100 reported in human melanomas.¹⁷ ASV-B mice also constitute a good model for hepatitis B virus-associated hepatocarcinoma. Indeed, HBx antigen, like T-SV40, could be the primary event in hepatic tumorigenesis, probably through its interaction with various cell cycle control proteins such as p53.¹⁸

In ASV-B mice the hepatocarcinoma develops progressively, thus the impact of immunointervention may be evaluated at different stages of the tumor. Because most patients enrolled in clinical oncology trials have failed standard therapies and thus generally present an advanced tumor by that time, we decided to investigate the effects of $\text{INF-}\gamma$ administration when the hepatocarcinoma was well established (at 4 months of age). Our results demonstrated that $\text{INF-}\gamma$ transfer, *via* the use of an adenovirus vector, resulted in the striking regression of hepatocarcinoma in a short period of time (7 days). In contrast to other studies,¹¹ no effect could be observed with the control

adenovirus, which is consistent with the absence of IFN- γ and STAT1 expression. Preliminary results concerning long-term therapy indicated a delay in the growth of the tumor after injection of Ad-IFN- γ , which lasted at least 3 weeks. But after this period, there was no more difference with control animals. This could be explained by the fact that as soon as the pressure of the treatment ceases, hepatocytes regenerate to repopulate the destroyed liver. With the ASV-B mice being transgenic, all the regenerating hepatocytes will express the oncogene upon maturation because it is under the control of antithrombin III promoter. In that context, hepatocytes repopulating the liver will go through the oncogenic process. For this reason, our model is not suited to evaluate neither long-term therapy nor mouse survival.

IFN- γ could act directly to induce tumor cell apoptosis. Various studies have demonstrated the antiproliferative and pro-apoptotic effects of this cytokine in various types of tumor cells.^{2,19} STAT1 has been shown to be implicated in these processes. Following activation, it binds to the promoter of the gene encoding the cyclin-dependent p21 kinase inhibitor, inducing its transcription.²⁰ Concurrently, activation of STAT1 signaling pathway has been shown to cause expression of Caspase 1 and apoptosis.²¹ Although cell lines derived from the hepatocarcinoma developed by ASV mice were found to be sensitive to IFN- γ ,¹⁵ and this correlated with STAT1 expression (data not shown), apoptosis was not observed. Indirect mechanisms should explain the apoptotic phenotype observed *in vivo*.

Numerous antitumor functions have been ascribed to IFN- γ , notably through its activation of innate and specific immune responses as well as its anti-angiogenic effects. At the time of sacrifice, no CD4 or CD8 T cells infiltrated the liver parenchyma, excluding a role of specific immune response. In contrast, macrophages probably play a major role in our model because transmigration through blood vessel walls and massive infiltration of hepatic parenchyma were observed in IFN- γ -treated mice. This accumulation could result from local proliferation of resident liver macrophages or alternatively to the recruitment of macrophages into the liver. Contribution of both processes seems to depend on the nature of the inflammatory stimuli.^{22,23,24} Our observations do not exclude one or the other mechanism. Importantly, damaged hepatocytes co-localized with macrophages. These cells were activated because iNOS and NO production was clearly increased. Activated macrophages have been reported to play a pivotal role in the selective detection and elimination of transformed cells.²⁵ The mechanisms involved are direct interaction with the tumor cell and secretion of cytotoxic molecules. In this context, IFN- γ up-regulates iNOS (as seen in our study), which in turn catalyzes the production of the pleiotropic agent, NO, in several cell types.²⁶ Controversial results have been described concerning the anti- or pro-apoptotic role of NO. It has been shown to inhibit the activity of Caspase 3, thus preventing apoptosis.²⁷ However, it has been shown to mediate down-regulation of Bcl2, an anti-apoptotic factor, in melanoma cells.²⁸ In fact, the final outcome seems to depend on the NO level and the pathway used in the target cell. Thus, NO would have a cytotoxic effect at high

concentration.²⁹ Our results showed that NO produced on Ad-IFN- γ treatment could be responsible, in part, for tumor cells destruction. Indeed, mortality of freshly isolated tumor hepatocytes was induced *in vitro* by SNP and DEA/NO, two NO releasing agents. Interestingly, tumor hepatocytes were more sensitive to NO activity than normal ones. Several studies also reported a tumoricidal role of NO *in vitro* and *in vivo*.^{30,31}

In a recent report, Fathallah-Shaykh et al¹² also observed a therapeutic effect of adenoviral-mediated gene transfer of IFN- γ in a mouse model of an established metastatic brain tumor. The antitumor effect was not due to immune-mediated response and was proven to be iNOS-independent. However, the authors did not observe any massive mononuclear infiltration at the tumor site in contrast to our primary hepatocarcinoma model. In these conditions, absence of iNOS role does not seem surprising. Nevertheless, they showed, using a 3LL-Matrigel assay *in vivo*, that Ad-IFN- γ injection inhibits neo-vascularization and apoptosis of endothelial cells. This last effect was not observed in our model. TUNEL-stained tissue sections showed that positive cells were mainly hepatocytes. This major difference could be linked to the model because hepatocarcinoma developed by our mice is probably less vascularized and thus less prompted to this kind of effects. However, we cannot exclude an anti-angiogenic role of IFN- γ mediated by other mechanisms.

Indeed, in the regulation of this process, numerous growth factors produced either by normal or transformed cells, such as FGF, TGF β , and VEGF, are known to be involved.^{32,33} Besides these factors, chemokines have also been implicated. Mig and IP-10 induced by IFN- γ have been described in several studies to be angiogenic inhibitor factors responsible for tumor regression.⁴⁻⁷ Detection of these factors in our model is under investigation. Previous results concerning TGF β production could be informative in understanding the mechanisms responsible for the observed destruction. During primary hepatocarcinoma development, there is a shift from TNF α mRNA to TGF β mRNA production, correlated with advanced stage of tumor growth.¹⁵ Hepatoma cell lines established *in vitro* from late hepatocarcinoma produce TGF β as well as VEGF proteins. Preliminary experiments have shown that treatment of these cells with IFN- γ results in down-regulation of TGF β and VEGF mRNA (data not shown). These results are consistent with previous studies demonstrating down-regulation of both factors in tumor cells by IFN- γ , possibly related to the inhibition of angiogenesis.^{10,34}

CONCLUSION

One major mechanism of tumor regression induced upon Ad-IFN- γ treatment seems to be NO production by infiltrated macrophages to which tumor cells are very sensitive. Altogether, data presented in this report support the use of IFN- γ recombinant adenovirus for treatment of primary liver cancers in clinical trials.



ACKNOWLEDGMENTS

We thank Maryline Tepper, Gilles Archangeli, and Manuel Lohez for their excellent technical assistance. We also thank Elodie Belnoue, as well as Ana Margarida Vigario, for helpful scientific discussions during this work.

This work was supported by grants from the French Ligue Nationale contre le Cancer, "axe immunologie des Tumeurs" program and from "Le comité de Paris."

REFERENCES

- Boehm U, Klamp T, Groot M, et al. Cellular responses to interferon- γ . *Annu Rev Immunol.* 1997;15:749–795.
- Xu X, Fu XY, Plate, et al. IFN- γ induces cell growth inhibition by Fas-mediated apoptosis: requirement of STAT1 protein for up-regulation of Fas and FasL expression. *Cancer Res.* 1998;58:2832–2837.
- Karavodin LM, Robbins J, Chong K, et al. Generation of a systemic antitumor response with regional intratumoral injections of interferon- γ retroviral vector. *Hum Gene Ther.* 1998;9:2231–2241.
- Siders WM, Wright PW, Hixon, et al. T cell- and NK cell-independent inhibition of hepatic metastases by systemic administration of an IL-12-expressing recombinant adenovirus. *J Immunol.* 1998;160:5465–5474.
- Arenberg DA, Kunkel SL, Polverini PJ, et al. Interferon- γ -inducible protein 10 IP-10 is an angiostatic factor that inhibits human non-small cell lung cancer NSCLC tumorigenesis and spontaneous metastases. *J Exp Med.* 1996;184:981–992.
- Sgadari C, Farber JM, Angiolillo AL, et al. Mig, the monokine induced by interferon- γ , promotes tumor necrosis *in vivo*. *Blood.* 1997;89:2635–2643.
- Coughlin CM, Salhany KE, Wysocka, et al. Interleukin-12 and interleukin-18 synergistically induce murine tumor regression which involves inhibition of angiogenesis. *J Clin Invest.* 1998;101:1441–1452.
- Kaplan DH, Shankaran V, Dighe AS, et al. Demonstration of an interferon- γ -dependent tumor surveillance system in immunocompetent mice. *Proc Natl Acad Sci USA.* 1998;95:7556–7561.
- Wilson JM. Cystic fibrosis. Vehicles for gene therapy [News]. *Nature.* 1993;365:691–692.
- Xu X, Dai Y, Heidenreich O, et al. Adenovirus-mediated interferon- γ transfer inhibits growth of transplanted HTLV-1 Tax tumors in mice. *Hum Gene Ther.* 1996;7:471–477.
- Zhang JF, Hu C, Geng Y, et al. Treatment of a human breast cancer xenograft with an adenovirus vector containing an interferon gene results in rapid regression due to viral oncolysis and gene therapy. *Proc Natl Acad Sci USA.* 1996;93:4513–4518.
- Fathallah-Shaykh HM, Zhao LJ, Kafrouni AI, et al. Gene transfer of IFN- γ into established brain tumors represses growth by anti-angiogenesis. *J Immunol.* 2000;164:217–222.
- Morel A, de La Coste A, Fernandez N, et al. Does preventive vaccination with engineered tumor cells work in cancer-prone transgenic mice? *Cancer Gene Ther.* 1998;5:92–100.
- Dubois N, Bennoun M, Allemand I, et al. Time course development of differentiated hepatocarcinoma and lung metastasis in transgenic mice. *J Hepatol.* 1991;13:227–239.
- Romieu R, Lacabanne V, Kayibanda, et al. Critical stages of tumor growth regulation in transgenic mice harboring a hepatocellular carcinoma revealed by distinct patterns of tumor necrosis factor-alpha and transforming growth factor-beta mRNA production. *Int Immunol.* 1997;9:1405–1413.
- Qin XQ, Tao N, Dergay A, et al. Interferon-beta gene therapy inhibits tumor formation and causes regression of established tumors in immune-deficient mice. *Proc Natl Acad Sci USA.* 1998;95:14411–14416.
- Van den Eynde BJ, Van der Bruggen P. T cell-defined tumor antigens. *Curr Opin Immunol.* 1997;9:684–693.
- Feitelson MA, Zhu M, Duan LX, et al. Hepatitis B antigen and p53 are associated *in vitro* and in liver tissues from patients with primary hepatocellular carcinoma. *Oncogene.* 1993;8:1109–1117.
- Kominsky S, Johnson HM, Bryan G, et al. IFN gamma inhibition of cell growth in glioblastomas correlates with increased levels of the cyclin-dependent kinase inhibitor p21WAF1/CIP1. *Oncogene.* 1998;17:2973–2979.
- Chin YE, Kitagawa M, Su WC, et al. Cell growth arrest and induction of cyclin-dependent kinase inhibitor p21 WAF1/CIP1 mediated by STAT1. *Science.* 1996;272:719–722.
- Chin YE, Kitagawa M, Kuida K, et al. Activation of the STAT signaling pathway can cause expression of Caspase 1 and apoptosis. *Mol Cell Biol.* 1997;17:5328–5337.
- Bouwens L, Baekland M, Wisse E. Importance of local proliferation in the expanding Kupffer cell population of rat liver after zymosan stimulation and partial hepatectomy. *Hepatol.* 1984;4:213–219.
- Pilaro AM, Laskin DL. Accumulation of activated mononuclear phagocytes in the liver following lipopolysaccharide treatment of rats. *J Leukocyte Biol.* 1986;40:29–41.
- Bouwens L, Knook DL, Wisse E. Local proliferation and extrahepatic recruitment of liver macrophages (Kupffer cells) in partial body irradiated rats. *J Leukocyte Biol.* 1986;39:687–697.
- Hibbs JB Jr, Lambert LH Jr, Remington JS. Control of carcinogenesis: a possible role for the activated macrophage. *Science.* 1972;177:998–1000.
- Kamijo R, Harada H, Matsuyama T, et al. Requirement for transcription factor IRF-1 in NO synthase induction in macrophages. *Science.* 1994;263:1612–1615.
- Li J, Billiar TR, Talanian RV, et al. Nitric oxide reversibly inhibits seven members of the Caspase family *via* S-nitrosylation. *Biochem Biophys Res Commun.* 1997;240:419–424.
- Xie K, Wang Y, Huang S, et al. Nitric oxide-mediated apoptosis of K-1735 melanoma cells is associated with down-regulation of Bcl-2. *Oncogene.* 1997;15:771–779.
- Hajri A, Metzger E, Vallat F, et al. Role of the nitric oxide in pancreatic tumour growth: *in vivo* and *in vitro* studies. *Br J Cancer.* 1998;78:841–849.
- Juang SH, Xie K, Xu L, et al. Suppression of tumorigenicity and metastasis of human renal carcinoma cells by infection with retroviral vectors harboring the murine inducible nitric oxide synthase gene. *Hum Gene Ther.* 1998;9:845–854.
- Kurose I, Higuchi H, Yonei Y, et al. Rat Kupffer cell-derived nitric oxide suppresses proliferation and induces apoptosis of syngeneic hepatoma cells. *Gastroenterology.* 1996;111:1058–1070.
- Folkman J, Klagsburn M. Angiogenic factors. *Science.* 1987;235:442–447.
- Risau W. Angiogenic growth factors. *Prog Growth Factor Res.* 1990;2:71–79.
- Dias S, Boyd R, Balkwill F. IL-12 regulates VEGF and MMPs in a murine breast cancer model. *Int J Cancer.* 1998;78:361–365.